**Materials and Methods**

*Zebrafish models*

Zebrafish were maintained according to protocols approved by the Committee on Animal Care at MIT. Experiments were performed in the AB/Tübingen (TAB5/14) genetic background and the *mitfa*$^{w2/w2}$ background which was derived by breeding the *roy* mutation out of casper zebrafish. *Tg(mitfa:GNAQ*$^{Q209L}$*);tp53*$^{-/-}$ zebrafish are the Q-1 transgenic line from (Perez et al., 2018). *Tg(mitfa:EGFP)* and *Tg(mitfa:YAP*$^{4A}$*;mitfa:EGFP)* transgenic lines were established by identifying germline founders from mosaic *Tg(mitfa:EGFP)* or mosaic *mitfa:YAP*$^{4A}$*;mitfa:GFP* zebrafish, respectively, by screening for GFP+ F1 progeny. F1 progeny were screened for single integration sites by southern blot analysis on DNA isolated from tail fin tissue samples obtained from adult F1 zebrafish anesthetized in 0.05% tricaine. Zebrafish were euthanized upon moribund tumor burden for Kaplan-Meier curves.

*Zebrafish larvae dissociation*

Zebrafish 5 dpf larvae (100-1,000 per sample) were anesthetized in 0.1% tricaine. Zebrafish eyes, which contained *Tg(mitfa:EGFP)*-expressing RPE contaminants, were removed by incubating whole bodies in TrypLE for 13-15min at 37ºC with vigorous shaking, then pipetted out, and the embryo bodies were collected. Bodies were dissociated in collagenase solution [1mg/mL collagenase, 1.25mg/mL BSA, 0.45mg/mL Soybean-Trypsin Inhibitor (STI), 0.1mg/mL DNase, in PBS] for 1 hour at 28ºC with vigorous shaking. Cells were stained with DAPI and filtered prior to analysis or sorting. Flow cytometry and FACS gates were as described in Higdon et al., 2013.

*RNA-sequencing and analysis*

Zebrafish tumor RNA-sequencing (RNA-seq) data (GSE190802) was from (Phelps et al., 2022). For zebrafish larval RNA-seq: zebrafish embryos were dissociated as described above. 30,000-100,000 *mitfa*:GFP+ cells were sorted on a BD FACSAria directly into 1ml of Trizol. During the sort the sample was vortexed every 10 minutes. Samples were stored at -80°C or directly used for RNA extraction. To extract RNA, 200 μL chloroform was added to the sample and briefly vortexed at medium speed. After resting 2 min at RT, the sample was centrifuged at 12,000 x g for 15 min at 4 °C. 400 μl of aqueous phase was removed and put into 1,400 μL RLT with 14 μL β-mercaptoethanol and mixed vigorously. 1,000 μL 100 % ethanol was added to each sample, mixed by pipetting, then loaded into RNeasy Micro Kit (Qiagen) columns. The manufacturer's directions were followed from the RW1 wash step and the sample was eluted into 14ul DEPC water.

Samples were analyzed for RNA integrity using a Femto Analyzer, and samples with a RIN > 8 were submitted for library prep. cDNA was prepared from 1 μL of total RNA using the SMART-Seq v4 Ultra Low Input RNA Kit (Takara) using 14 cycles of amplification. Resulting cDNA were confirmed using a Fragment Analyzer and Illumina libraries prepared using NexteraXT (Illumina) and sequenced on a HiSeq2000 (Illumina) using 40nt single end reads.

RNA-seq data was used to quantify transcripts from the zv11 zebrafish assembly with the Ensembl version 104 annotation using Salmon version 1.3.0 (Patro et al., 2017). Gene level summaries were prepared using tximport version 1.20.0 (Soneson et al., 2015) running under R version 4.1.0 (R Core Team, 2021). Differential expression analysis was conducted with DESeq2 version 1.32.0 (Anders & Huber, 2010; Love et al., 2014) and differentially expressed genes defined as those having an absolute apeglm (Zhu et al., 2019) log2 fold change greater than 1 and an adjusted p-value less than 0.05. Data parsing and clustering was conducted using Tibco Spotfire Analyst 11.4.0. Zebrafish genes were mapped to human orthologs as described previously (Zhang et al., 2013) and preranked Gene Set Enrichment Analysis (Mootha et al., 2003) conducted using javaGSEA version 4.1.0 with msigDb version 7.4 (Subramanian et al., 2005) gene sets. RNA-seq data are available from the Gene Expression Omnibus under the accession number GSE197927.

Combined z-scores were calculated for specific gene lists (Howard et al., 2021; Table S1) by calculating the z-score for each zebrafish gene across each of the RNA-seq samples, and summing the z-scores for each gene in the gene list for each sample.

*TCGA analysis*

RNA-sequencing of primary tumors and corresponding survival data were obtained from The Cancer Genome Atlas (TCGA) PanCancer Atlas database of uveal melanoma (UVM; n = 80 patients). Z-scores were calculated for each queried gene across each patient in the mRNA expression, RSEM, batch normalized from Illumina HiSeq_RNAseqV2 RNA-seq dataset.

*Chemical inhibitor assays*

The general scheme is depicted in Figure 3C. Zebrafish were placed in tissue culture-treated dishes and treated at 2.5 dpf with chemical inhibitors dissolved in DMSO at the maximum tolerated dose, unless otherwise indicated. Chemical inhibitor (dose): **Verteporfin** (25μg/mL; maximum soluble dose), **PND-1186** (5μM), **Trametinib** (200nM), **Ly294002** (2.5μM). No overt developmental defects were observed with this dosing scheme. Zebrafish treated with verteporfin were always kept in the dark because verteporfin is photoreactive. Zebrafish were dissociated at 5 dpf as described above and *mitfa:EGFP* positivity was analyzed by flow cytometry. Samples were derived from an intercross of zebrafish with

and without the *mitfa:EGFP* reporter, and thus roughly half of the larval zebrafish contain the *mitfa:EGFP* reporter.

*Statistical analyses*

Prism software was used to analyze data, draw graphs, and perform statistical analyses. Log-rank tests were used for Kaplan-Meier/survival curves. All other statistical analyses were performed using Student's unpaired *t*-test. Data are presented as mean ± SD (error bars). For statistical significance, *$p \leq 0.05$, **$p \leq 0.01$, ***$p \leq 0.001$, and ****$p \leq 0.0001$ were considered significant, n.s. refers to not significant ($p > 0.05$).

**Supplemental Figures**

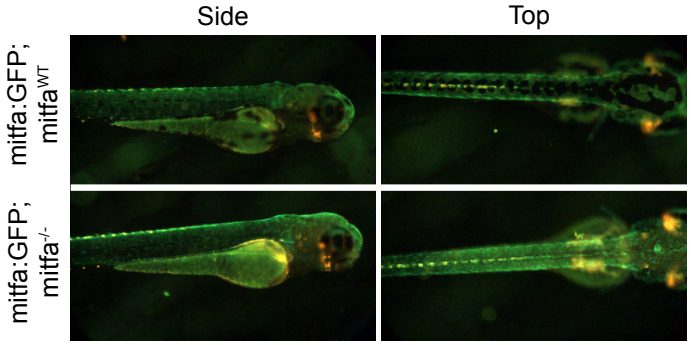


**Figure S1. *Tg(mitfa:EGFP);mitfa$^{-/-}$* zebrafish embryos express widespread GFP, similar to *Tg(mitfa:EGFP) mitfa$^{WT}$*.** Image of zebrafish embryos (3dpf), top & side views. As previously reported (Johnson et al., 2011; Phelps et al., 2022), *Tg(mitfa:EGFP);mitfa$^{-/-}$* appear to express brighter GFP, likely because pigmentation could block GFP signal.

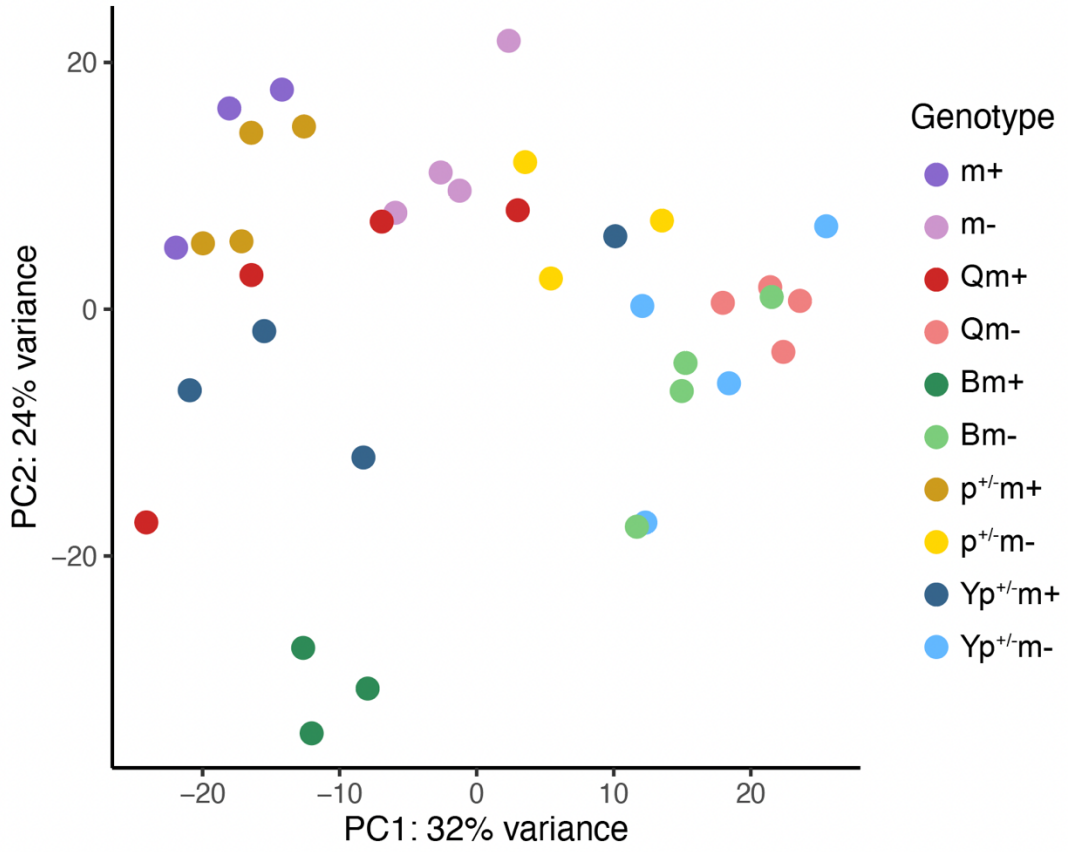


**Figure S2. RNA-sequencing replicates from larval melanocyte lineage cells largely cluster with each other.** Principal component analysis (PCA) on all larval *mitfa:EGFP* RNA-sequencing samples, which express $GNAQ^{Q209L}$, $BRAF^{V600E}$, or $YAP^{AA}$ or no oncogene controls, with or without *mitfa*-deficiency. Genotype abbreviations are as follows: *Tg(mitfa:EGFP)* (m+), *Tg(mitfa:EGFP);mitfa*$^{-/-}$ (m-), *Tg(mitfa:GNAQ*$^{Q209L}$*);Tg(mitfa:EGFP)* (Qm+), *Tg(mitfa:GNAQ*$^{Q209L}$*);Tg(mitfa:EGFP);mitfa*$^{-/-}$ (Qm-), *Tg(mitfa:BRAF*$^{V600E}$*);Tg(mitfa:EGFP)* (Bm+), *Tg(mitfa:BRAF*$^{V600E}$*);Tg(mitfa:EGFP);mitfa*$^{-/-}$ (Bm-), *Tg(mitfa:EGFP);tp53*$^{+/-\ or\ +/+}$ ($p^{+/-}$m+), *Tg(mitfa:EGFP);tp53*$^{+/-\ or\ +/+}$*;mitfa*$^{-/-}$ ($p^{+/-}$m-), *Tg(mitfa:YAP*$^{AA}$*;mitfa:EGFP);tp53*$^{+/-\ or\ +/+}$ ($Yp^{+/-}$m+), *Tg(mitfa:YAP*$^{AA}$*;mitfa:EGFP);tp53*$^{+/-\ or\ +/+}$*;mitfa*$^{-/-}$ ($Yp^{+/-}$m-).

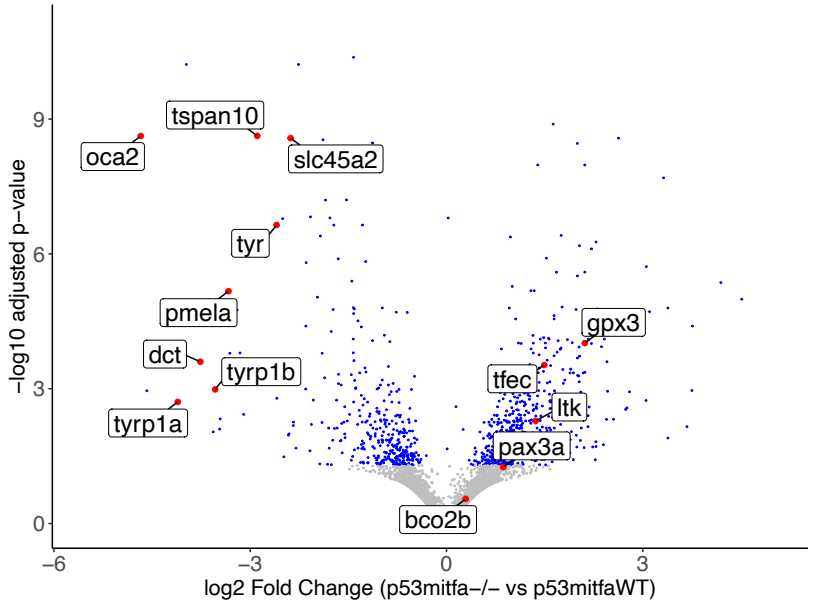


**Figure S3. *mitfa*-deficient melanocyte lineage cells still down-regulate melanocyte differentiation genes, and up-regulate pigment progenitor or neural crest-associated genes, in a *tp53*$^{+/-}$ background.** Volcano plot depicting differentially expressed genes between p$^{+/-}$m- and p$^{+/-}$m+ larval cells. Statistically significant (adjusted p-value < 0.05) genes in blue or red (if labeled), statistically insignificant (adjusted p-value > 0.05) in grey.

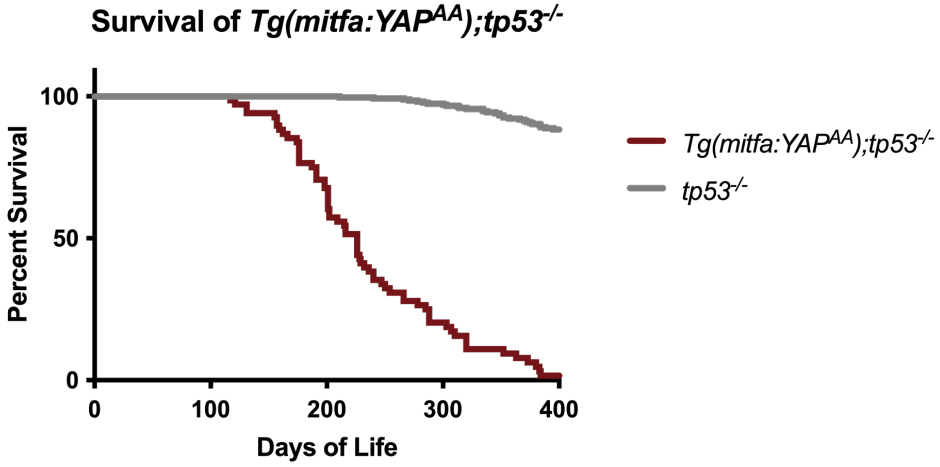


**Figure S4. Germline *Tg(mitfa:YAP*$^{AA}$*)* drives tumorigenesis in a *tp53*-null background.** Kaplan-Meier curve of overall survival of *Tg(mitfa:YAP*$^{AA}$*);tp53*$^{-/-}$ zebrafish compared to *tp53*$^{-/-}$.

**References**


Anders, S., & Huber, W. (2010). Differential expression analysis for sequence count data. *Genome Biology*, *11*(10), R106. https://doi.org/10.1186/gb-2010-11-10-r106

Higdon, C. W., Mitra, R. D., & Johnson, S. L. (2013). Gene Expression Analysis of Zebrafish Melanocytes, Iridophores, and Retinal Pigmented Epithelium Reveals Indicators of Biological Function and Developmental Origin. *PLOS ONE*, *8*(7), e67801. https://doi.org/10.1371/journal.pone.0067801

Howard, A. G., IV, Baker, P. A., Ibarra-García-Padilla, R., Moore, J. A., Rivas, L. J., Tallman, J. J., Singleton, E. W., Westheimer, J. L., Corteguera, J. A., & Uribe, R. A. (2021). An atlas of neural crest lineages along the posterior developing zebrafish at single-cell resolution. *ELife*, *10*, e60005. https://doi.org/10.7554/eLife.60005

Johnson, S. L., Nguyen, A. N., & Lister, J. A. (2011). Mitfa is required at multiple stages of melanocyte differentiation but not to establish the melanocyte stem cell. *Developmental Biology*, *350*(2), 405–413. https://doi.org/10.1016/j.ydbio.2010.12.004

Love, M. I., Huber, W., & Anders, S. (2014). Moderated estimation of fold change and dispersion for RNA-seq data with DESeq2. *Genome Biology*, *15*(12), 550. https://doi.org/10.1186/s13059-014-0550-8

Mootha, V. K., Lindgren, C. M., Eriksson, K.-F., Subramanian, A., Sihag, S., Lehar, J., Puigserver, P., Carlsson, E., Ridderstråle, M., Laurila, E., Houstis, N., Daly, M. J., Patterson, N., Mesirov, J. P., Golub, T. R., Tamayo, P., Spiegelman, B., Lander, E. S., Hirschhorn, J. N., … Groop, L. C. (2003). PGC-1α-responsive genes involved in oxidative phosphorylation are coordinately downregulated in human diabetes. *Nature Genetics*, *34*(3), 267–273. https://doi.org/10.1038/ng1180

Patro, R., Duggal, G., Love, M. I., Irizarry, R. A., & Kingsford, C. (2017). Salmon provides fast and bias-aware quantification of transcript expression. *Nature Methods*, *14*(4), 417–419. https://doi.org/10.1038/nmeth.4197

Perez, D. E., Henle, A. M., Amsterdam, A., Hagen, H. R., & Lees, J. A. (2018). Uveal melanoma driver mutations in GNAQ/11 yield numerous changes in melanocyte biology. *Pigment Cell & Melanoma Research*, *31*(5), 604–613. https://doi.org/10.1111/pcmr.12700

Phelps, G. B., Hagen, H. R., Amsterdam, A., & Lees, J. A. (2022). MITF deficiency accelerates GNAQ-driven uveal melanoma. *Proceedings of the National Academy of Sciences*, *119*(19), e2107006119. https://doi.org/10.1073/pnas.2107006119

R Core Team. (2021). *R: A Language and Environment for Statistical Computing*. R Foundation for Statistical Computing. https://www.R-project.org

Soneson, C., Love, M. I., & Robinson, M. D. (2015). Differential analyses for RNA-seq: Transcript-level estimates improve gene-level inferences. *F1000Research*, *4*, 1521. https://doi.org/10.12688/f1000research.7563.2

Subramanian, A., Tamayo, P., Mootha, V. K., Mukherjee, S., Ebert, B. L., Gillette, M. A., Paulovich, A., Pomeroy, S. L., Golub, T. R., Lander, E. S., & Mesirov, J. P. (2005). Gene set enrichment analysis: A knowledge-based approach for interpreting genome-wide expression profiles. *Proceedings of the National Academy of Sciences*, *102*(43), 15545–15550. https://doi.org/10.1073/pnas.0506580102

Zhang, G., Hoersch, S., Amsterdam, A., Whittaker, C. A., Beert, E., Catchen, J. M., Farrington, S., Postlethwait, J. H., Legius, E., Hopkins, N., & Lees, J. A. (2013). Comparative Oncogenomic Analysis of Copy Number Alterations in Human and Zebrafish Tumors Enables Cancer Driver Discovery. *PLOS Genetics*, *9*(8), e1003734. https://doi.org/10.1371/journal.pgen.1003734

Zhu, A., Ibrahim, J. G., & Love, M. I. (2019). Heavy-tailed prior distributions for sequence count data: Removing the noise and preserving large differences. *Bioinformatics*, *35*(12), 2084–2092. https://doi.org/10.1093/bioinformatics/bty895